Nonlinear Oscillations in Biology and Chemistry. Lect Notes - Biomath, 66, pp46-65, Springer (1986)

# AN ANALYSIS OF ONE- AND TWO-DIMENSIONAL PATTERNS IN A MECHANICAL MODEL FOR MORPHOGENESIS

by

P. K. Maini and J. D. Murray
Centre for Mathematical Biology
Mathematical Institute
University of Oxford
Oxford OX1 3LB

G. F. Oster
Department of Biophysics
University of California
Berkeley, CA 94720

ABSTRACT

In early embryonic development, fibroblast cells move through an extracellular matrix (ECM) exerting large traction forces which deform the ECM. We model these mechanical interactions mathematically and show that the various effects involved can combine to produce pattern in cell density. A linear analysis exhibits a wide selection of dispersion relations, suggesting a richness in pattern forming capability of the model. A nonlinear bifurcation analysis is presented for a simple version of the governing field equations. The one-dimensional analysis requires a non-standard element. The two-dimensional analysis shows the possibility of roll and hexagon pattern formation. A realistic biological application to the formation of feather germ primordia is briefly discussed.



## 1. Introduction.

Several models have been proposed to describe the mechanisms involved in morphogenesis - the development of biological pattern and form. The majority of these view morphogenesis as a two stage process. In the first, a pre-pattern is set up in some chemical (morphogen) concentration. In the second, cells respond to the local concentration of morphogen and differentiate according to their 'positional information' (Wolpert (1969), (1981)).

The pre-pattern may be set up by simple diffusion or in a typical Turing reaction-diffusion way (Turing (1952), Murray (1977),(1981 a,b), Meinhardt (1982), Tickle et al (1975), Wolpert et al (1971)).

An alternative approach has been made by Oster et al (1983, 1985) and Murray and Oster (1984 a, b), based on the following experimental observations (Harris et al (1981)): 1) cells spread and migrate within a substratum consisting of a fibrous extracellular matrix and 2) they generate large contractile forces which deform the ECM.

For completeness, section 2 contains a brief derivation of the model equations (see Oster et al (1983) for fuller details). In section 3 the results of a linear analysis are given which show the wide selection of dispersion relations possible. In section 4, we carry out a nonlinear bifurcation analysis on a simple but practical version of the model. In section 5, we investigate two dimensional patterns in a caricature of the model analyzed in section 4, and show the possibility of roll and hexagonal structure in cell density populations. Finally, we briefly discuss the biological application to the problem of feather germ formation.

## 2. Model Equations.

The model is based on the three field variables:

$n(\underline{x},t)$ = density of mesenchymal cells at position $\underline{x}$ and time t.

$\rho(\underline{x},t)$ = density of ECM at position $\underline{x}$ and time t.

$\underline{u}(\underline{x},t)$ = displacement at time t of a material point in the matrix initially at $\underline{x}$.

The model equations are:

Cell conservation: $\frac{\partial n}{\partial t} = \nabla\cdot[D_1\nabla n - D_2\nabla^3 n - \alpha n\nabla\rho - n\frac{\partial u}{\partial t}] + rn(N-n)$ (2.1a)

Mechanical balance: $\nabla\cdot[\mu_1\frac{\partial\varepsilon}{\partial t} + \mu_2\frac{\partial\theta}{\partial t}\mathrm{I} + \frac{E}{1+\nu}\{\varepsilon + \hat{\nu}\theta\mathrm{I}\}$

$+ \frac{\tau n}{(1+\lambda n^2)}\{\rho + \beta\nabla^2\rho\}\mathrm{I}] = su\rho$ (2.1b)

Matrix conservation: $\frac{\partial\rho}{\partial t} + \nabla\cdot\{\rho\,\frac{\partial u}{\partial t}\} = 0$ (2.1c)

where $\varepsilon = \frac{1}{2}\{\nabla u + \nabla u^T\}$ is the linear strain tensor and $D_1$, $D_2$, $\alpha$, r, N, $\mu_1$, $\mu_2$, E, $\nu$, $\hat{\nu}$, $\lambda$, $\tau$ and $\beta$ are parameters which we describe below.

We briefly motivate the various contributions to equations (2.1a)-(2.1c).

Cell conservation. The equation for cell conservation is of the form

$$\frac{\partial n}{\partial t} = -\nabla\cdot\underline{J} + rn(N-n) \qquad (2.2)$$

where $\underline{J}$ is the cell flux through a volume element of matrix and, to be specific, we have taken a logistic growth term where r, the mitotic rate, and N are positive constants. The cell flux, $\underline{J}$, is made up of a number of terms:

Random dispersal: In populations of low cell density, random dispersal of cells may be modelled with a Fickian flux $-D_1\nabla n$ where $D_1$ is the diffusion coefficient. However, with high mesenchymal cell densities, we should take non-local effects into account since mesenchymal cells have long finger-like extensions (filopodia) which can detect non-local cell densities. Thus cell 'diffusion' depends also on the average cell density in the immediate surrounding. We model this non-local (long range) diffusion by $D_2\nabla(\nabla^2 n)$ where $D_2$ is the coefficient of long range diffusion.

Haptotaxis. Cells actively move by attaching their filopodia to adhesive sites in the ECM. The tendency of cells to move up a gradient in adhesive sites (Harris (1973)) is called haptotaxis. Assuming, reasonably, that the density of adhesive sites is proportional to the matrix density, we model the haptotactic flux as $\alpha n\nabla\rho$ where $\alpha$ is the coefficient of haptotaxis. We could, of course,



include a long range haptotactic effect but for simplicity do not do so here.

Convection. Cells are passively carried on the substratum and this convective motion is given by $n\,\frac{\partial u}{\partial t}$. Here $\frac{\partial u}{\partial t}$ is the velocity. This is probably the most important dispersal component.

Substituting these contributions into (2.2) gives (2.1a)

Mechanical balance. We are dealing with systems with very low Reynolds number (Purcell (1977), Odell et al (1981)) so the viscous and elastic forces dominate the inertial terms and cell motion instantly ceases when the applied forces are turned off. Therefore there is a balance between the cell contractile forces deforming the ECM and the viscous and elastic restoring forces in the ECM. There is experimental evidence for assuming small strains. We therefore model the cell-matrix composite as a linear, isotropic, viscoelastic material with stress tensor $\sigma = \sigma_{matrix} + \sigma_{cell\text{-}matrix}$, where

$$\sigma_{matrix} = \underbrace{\mu_1\frac{\partial\varepsilon}{\partial t} + \mu_2\frac{\partial\theta}{\partial t}\mathrm{I}}_{\text{viscous}} + \underbrace{\frac{E}{1+\nu}\{\varepsilon + \hat{\nu}\theta\mathrm{I}\}}_{\text{elastic}},$$

where $\theta = \operatorname{div}\underline{u}$, the dilatation, E is Young's modulus, $\mu_1$ and $\mu_2$ the shear and bulk viscosities respectively, $\nu$ the Poisson ratio, $\hat{\nu} = \frac{\nu}{1-2\nu}$, and I the unit tensor.

The stress due to the contractile forces exerted by the cells is taken as $\sigma_{cell\text{-}matrix} = \tau(n)n[\rho+\beta\nabla^2\rho]\mathrm{I}$ where $\tau(n) = \frac{\tau}{1+\lambda n^2}$ is the traction/unit length/unit cell, $\tau$, $\lambda$ and $\beta$ are positive constants. The motivation for this term is that mesenchymal cells exert contractile forces by attaching their filopodia to the adhesive sites and compressing the matrix. Therefore, the contractile force is proportional to the density of adhesive sites which in turn, we take as proportion to $\rho$. Long range effects should again be taken into account: this gives the term $\beta\nabla^2\rho$. As cell density increases, the traction/unit cell decreases due to cell-cell inhibition (Trinkaus (1984)), hence the qualitative form of $\tau(n)$ taken. The equation for mechanical equilibrium is

$$\nabla\cdot\sigma + \rho\underline{F} = \underline{0}$$

where $\underline{F}$ is a body force. Typically the ECM is attached elastically to a subdermal layer which we model as a linear spring and so $\underline{F} = -s\underline{u}$, where s is a positive constant.

Matrix conservation. The matrix density $\rho$ satisfies the usual conservation equation

$$\frac{\partial \rho}{\partial t} + \nabla \cdot \{\rho \frac{\partial \underline{u}}{\partial t}\} = 0$$

With the processes and time scales we are concerned with here no matrix is being secreted.

## 3. Linear Dispersion Relations.

It is convenient to non-dimensionalise the system to highlight the dimensionless parameter groupings in a biologically significant way: they indicate which biological processes have equivalent effects. The system reduces to

$$\frac{\partial n}{\partial t} = D_1 \nabla^2 n - D_2 \nabla^4 n - \alpha \nabla \cdot \{n \nabla \rho\} - \nabla \cdot \{n \frac{\partial \underline{u}}{\partial t}\} + rn(1-n) \qquad (3.1a)$$

$$\nabla \cdot [\mu_1 \frac{\partial \varepsilon}{\partial t} + \mu_2 \frac{\partial \theta}{\partial t} I + (\varepsilon + \hat{\nu}\theta I) + \frac{\tau n}{(1+\lambda n^2)} \{\rho + \beta \nabla^2 \rho\} I] = s\underline{u}\rho \qquad (3.1b)$$

$$\frac{\partial \rho}{\partial t} + \nabla \cdot \{\rho \frac{\partial \underline{u}}{\partial t}\} = 0 \qquad (3.1c)$$

where $D_1$, $D_2$, $\alpha$, $r$, $\mu_1$, $\mu_2$, $\lambda$, $\beta$, $\tau$ and $s$ are non-dimensional parameter groupings (see Appendix (A.1)).

Linearising about the biologically relevant steady state $n = 1 = \rho$, $\underline{u} = \underline{0}$ in the usual way we obtain the dispersion relation for the growth rate $\sigma$ as a function of the wave number k. (Appendix (A.2)).

Setting various parameters equal to zero gives rise to varied behaviour for $\sigma(k^2)$: Table 1 illustrates a few of these. Spatial patterns evolve when the parameters are such that $R\ell\sigma(k^2) > 0$, $k^2 \neq 0$.



**Table 1:** (a) Examples of possible types of dispersion relation $\sigma(k^2)$ (Appendix (A.2)) with finite ranges of unstable k (wave number) in the case $\lambda = \beta = 0$.

+++ denotes unstable wave number
● denotes non-zero parameter
○ denotes parameter set to zero

| $D_1$ | $D_2$ | $\alpha$ | r | $\mu$ | s | Conditions on $\tau$ | $\sigma(k^2)$ |
|---|---|---|---|---|---|---|---|
| ● | ○ | ○ | ○ | ● | ● | $1/2 + \mu D_1 s < \tau < 1$ | 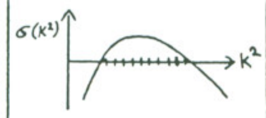 |
| ● | ○ | ○ | ○ | ● | ○ | $1/2 < \tau < 1$ | 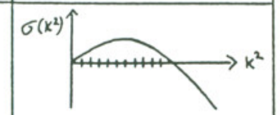 |
| ● | ● | ● | ○ | ○ | ● | $(D_1 + sD_2)/(D_1 + \alpha) < \tau < 1/2$<br>$[(D_1 + \alpha)\tau - (D_1 + sD_2)]^2 > 4sD_1D_2(1 - \tau)$ | 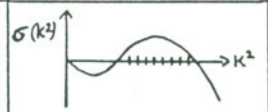 |
| ○ | ● | ● | ○ | ○ | ● | $\tau > \max[1, sD_2/\alpha]$ | 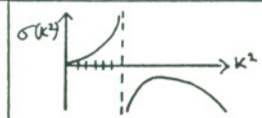 |
| ● | ● | ● | ● | ○ | ● | $1/2 < \tau < 1$<br>+ quadratic condition on $\tau$ | 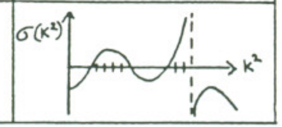 |

(b) Examples of the dispersion relation $\sigma(k^2)$ (Appendix (A.2)) with infinite ranges of unstable k (wave number) in the case $\lambda = \beta = 0$.

| $D_1$ | $D_2$ | $\alpha$ | $\tau$ | $\mu$ | s | Conditions on $\tau$ | $\sigma(k^2)$ |
|---|---|---|---|---|---|---|---|
| ● | ● | ● | ○ | ○ | ● | $1/2 < \tau < 1$<br>$\tau > (D_1 + sD_2)/(D_1 + \alpha)$<br>+ two quadratic conditions on $\tau$ | 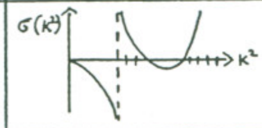 |
| ● | ● | ● | ○ | ○ | ● | $1/2 < \tau < 1$<br>$\tau > (D_1 + sD_2)/(D_1 + \alpha)$<br>+ two quadratic conditions on $\tau$ | 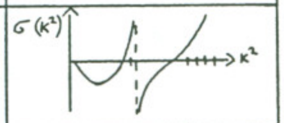 |
| ○ | ● | ● | ○ | ○ | ● | $1/2 + sD_2/2\alpha < \tau < 1$<br>$\tau > sD_2/\alpha$ | 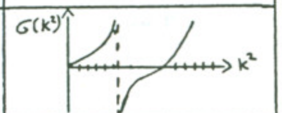 |
| ● | ● | ● | ● | ○ | ● | $\tau < 1/2$<br>+ condition that $c(k^2)=0$ has 3 real roots |  |
| ○ | ● | ● | ○ | ○ | ● | $1/2 < \tau < 1/2 + sD_2/2\alpha$ | 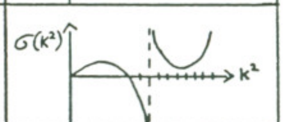 |
| ○ | ○ | ○ | ● | ● | ● | $1 < \tau < (\mu r + 1)/2$ | 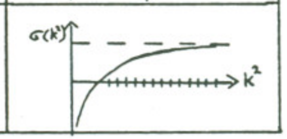 |

[The form of some of these dispersion relations indicates the lack of validity of a linear theory.]



## 4. One-Dimensional Nonlinear Analysis.

In this section we briefly summarize some results from Maini et al (1984) for a simple version of the model of biological relevance in which $\tau$, $\mu$, $\beta$, and s are the only non-zero parameters. We take $\tau$ to be the bifurcation parameter. The one-dimensional system we consider is

$$\frac{\partial n}{\partial t} + \frac{\partial}{\partial x}\left\{n\frac{\partial u}{\partial t}\right\} = 0 \tag{4.1a}$$

$$\frac{\partial^3 u}{\partial x^2 \partial t} + \frac{\partial^2 u}{\partial x^2} + \tau\frac{\partial}{\partial x}\left[n\left\{\rho + \beta\frac{\partial^2 \rho}{\partial x^2}\right\}\right] - su\rho = 0 \tag{4.1b}$$

$$\frac{\partial \rho}{\partial t} + \frac{\partial}{\partial x}\left\{\rho\frac{\partial u}{\partial t}\right\} = 0 \tag{4.1c}$$

where we have rescaled time by dividing through by $\mu$.

The dispersion relation (from (A.2)) is

$$\sigma = 0,\ \sigma(k^2) = -\frac{\beta\tau k^4 + (1-2\tau)k^2 + s}{k^2} \tag{4.2}$$

The trivial solution corresponds to neutral stability of the steady state and is not considered in the following analysis. Figure 1 illustrates the behaviour of the dispersion relation as $\tau$ increases.

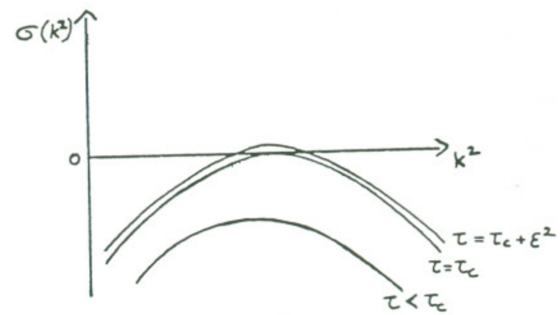


**Figure 1.** Behaviour of the non-zero solution for $\sigma(k^2)$ (see(4.2)) as $\tau$ increases. There is a critical value for $\tau$ ($\tau_c$) such that if $\tau < \tau_c$, the uniform steady state ($n = \rho = 1$, $u = 0$) is stable. For $\tau = \tau_c + \varepsilon^2$ ($0 < \varepsilon \ll 1$) the uniform steady state is unstable and spatial disturbances of wave number $k_c$ grow fastest where $k_c^2 = \sqrt{\frac{s}{\beta\tau_c}}$ and $\tau_c = \frac{1}{2}\left[1+s\beta+\sqrt{(1+s\beta)^2-1}\right]$.

Linear analysis therefore, predicts that if $\tau = \tau_c + \varepsilon^2\delta$, where $0 < \varepsilon < 1$ and $\delta = +1$, then the uniform steady state goes unstable and the fastest growing unstable wave number is $k_c$, where

$$\tau_c = \frac{1}{2}\left[1+s\beta+\sqrt{(1+s\beta)^2-1}\,\right] \quad \text{and} \quad k_c^2 = \sqrt{\frac{s}{\beta\tau_c}} \tag{4.3}$$

Expanding $\sigma$ about $(k_c^2,\tau)$ in a Taylor series we have

$$\sigma(k_c^2,\tau_c + \varepsilon^2\delta) = \cancelto{0}{\sigma(k_c^2,\tau_c)} + \varepsilon^2\delta\left.\frac{\partial\sigma}{\partial\tau}\right|_{k_c^2,\tau_c} + 0(\varepsilon^4) \tag{4.4}$$

Thus the exponential growth term is $\exp(0(\varepsilon^2)t)$ and this suggests the usual long time scale $T = \varepsilon^2 t$ (Lara Ochoa and Murray (1983)). As $k_c$ is the fastest growing wave number, we assume that on the long time scale T, the nonlinear solution will have wave number $k_c$ (Matkowsky (1970)). To investigate the nonlinear behaviour of (4.1a)-(4.1c), we use the method of balancing harmonics and substitute

$$n(x,T,\varepsilon) = 1 + \sum_{j=1} \varepsilon^j\{A_j(\varepsilon,T)\cos jk_cx + D_j(\varepsilon,T)\sin jk_cx\}$$

$$u(x,T,\varepsilon) = \sum_{j=1} \varepsilon^j\{B_j(\varepsilon,T)\sin jk_cx + E_j(\varepsilon,T)\cos jk_cx\}$$

$$\rho(x,T,\varepsilon) = 1 + \sum_{j=1} \varepsilon^j\{C_j(\varepsilon,T)\cos jk_cx + F_j(\varepsilon,T)\sin jk_cx\} \tag{4.5}$$

where $T = \varepsilon^2 t$ and $A_j = \sum_{i=0} A_j^i(T)\varepsilon^i$, etc.

into (4.1a)-(4.1c) and equate coefficients of $\varepsilon$. This leads to a hierachy of <u>linear</u> equations for the coefficients $A_j^i(T)$, $B_j^i(T)$, $C_j^i(T)$, $D_j^i(T)$, $E_j^i(T)$ and $F_j^i(T)$ which we can solve. To lowest order in $\varepsilon$, we have

$$\frac{d}{dT}\left(A_1^0(T) + k_cB_1^0(T)\right) = 0$$

$$k_c\tau_cA_1^0(T) + (k_c^2+s)B_1^0(T) + k_c\tau_c(1-k_c^2\beta)C_1^0(T) = 0 \tag{4.6}$$

$$\frac{d}{dT}\left(C_1^0(T) + k_cB_1^0(T)\right) = 0$$

and a similar set of equations for $\{D_1^0(T), E_1^0(T), F_1^0(T)\}$. For the remaining calculation we shall only consider $\{A_j^i(T), B_j^i(T), C_j^i(T)\}$ to simplify the analysis. The analysis may be repeated exactly for $\{D_j^i(T), E_j^i(T), F_j^i(T)\}$.

Order $\varepsilon^2$ terms give

$$\frac{d}{dT}\{A_2^0(T) + 2k_cB_2^0(T)\} + k_cA_1^0(T)\frac{dB_1^0(T)}{dT} = 0$$

$$2k_c\tau_cA_2^0(T) + (4k_c^2+s)B_2^0(T) + 2k_c\tau_c(1-4\beta k_c^2)C_2^0(T) =$$

$$-k_c\tau_c(1-\beta k_c^2)A_1^0(T)C_1^0(T) - \frac{s}{2}B_1^0(T)C_1^0(T) \tag{4.7}$$

$$\frac{d}{dT}\{C_2^0(T) + 2k_cB_2^0(T)\} + k_cC_1^0(T)\frac{dB_1^0(T)}{dT} = 0$$

and at order $\varepsilon^3$, (4.1b) gives

$$-k_c\frac{dB_1^0(T)}{dT} + k_c\delta\{A_1^0(T) + C_1^0(T)\} + \beta\delta k_c^3C_1^0(T) +$$

$$k_c\tau_c(2\beta k_c^2 - \tfrac{1}{2})A_1^0(T)C_2^0(T) + \frac{k_c\tau_c}{2}\{\beta k_c^2 - 1\}A_2^0(T)C_1^0(T) \tag{4.8}$$

$$-\frac{s}{2}\{C_1^0(T)B_2^0(T) - B_1^0(T)C_2^0(T)\} = 0$$

Standard nonlinear analysis simply requires successive suppression of secular terms. With the structure of our equations this is <u>not</u> sufficient to determine the amplitude equations. We have to use an <u>integrated</u> form of the conservation equations. Integrating the first and third of (4.6) we have three simultaneous equations for $A_1^0(T)$, $B_1^0(T)$ and $C_1^0(T)$, namely

$$A_1^0(T) + k_cB_1^0(T) = \gamma_1^0$$

$$k_c\tau_cA_1^0(T) + (k_c^2+s)B_1^0(T) + k_c\tau_c(1-\beta k_c^2)C_1^0(T) = 0 \tag{4.9}$$

$$k_cB_1^0(T) + C_1^0(T) = \gamma_3^0$$

where $\gamma_1^0$ and $\gamma_3^0$ are constants. The system (4.9) is degenerate and has nontrivial solution if and only if

$$[k_c^2(1-\tau_c) + s]\gamma_3^0 + k_c^2\tau_c\gamma_1^0 = 0 \tag{4.10}$$

that is, there is a <u>constraint</u> on the initial conditions. This is what we would expect because of the intimate relationship between $u(x,t)$ and $\rho(x,t)$.

Integrating the first and third of (4.7) gives

$$A_2^0(T) + 2k_c B_2^0(T) = \frac{\{A_1^0(T)\}^2}{2} + \gamma_1^1$$
$$C_2^0(T) + 2k_c B_2^0(T) = \frac{\{C_1^0(T)\}^2}{2} + \gamma_3^1 \qquad (4.11)$$

where $\gamma_1^1$ and $\gamma_3^1$ are constants.

Note that $\gamma_1^0 = A_1^0(0) + k_c B_1^0(0)$. If we assume initial perturbations to be $O(\varepsilon^2)$, then $\gamma_1^0 = \gamma_3^0 = 0$. Moreover, assuming initial perturbations to be $O(\varepsilon^3)$ implies $\gamma_1^1 = \gamma_3^1 = 0$. Making these assumptions is not necessary but they simplify the analysis.

We solve system (4.9) and the integrated form of (4.7) for $B_1^0(T)$, $C_1^0(T)$, $A_2^0(T)$, $B_2^0(T)$ and $C_2^0(T)$ in terms of $A_1^0(T)$ and, substituting into (4.8), we have the usual Landau equation

$$\frac{dA_1^0(T)}{dT} = \delta X A_1^0(T) + Y\{A_1^0(T)\}^3 \qquad (4.12)$$

where $X = \dfrac{2\tau_c+1}{2\tau_c}$ and $Y = \dfrac{\{14\beta s\tau_c + 24\tau_c - 63\beta s - 12\}}{72\beta s}$

The behaviour of (4.12) is summarised in Table 2.



**Table 2.** Behaviour of $A_1^0(T)$ from equation (4.12).

| | $Y < 0$ | $Y > 0$ |
|---|---|---|
| $\delta > 0$ | $A_1^0$ evolves to $\{X/\lvert Y\rvert\}^{1/2}$ | $A_1^0 \to \infty$ |
| $\delta < 0$ | $A_1^0 \to 0$ | Threshold in $A_1^0(0)$: $A_1^0(0) < \{X/Y\}^{1/2} \Rightarrow A_1^0 \to 0$; $A_1^0(0) > \{X/Y\}^{1/2} \Rightarrow A_1^0 \to \infty$ |

If we are in the parameter space P (Figure 2) the cell density evolves to the bounded steady state

$$n = 1 + \varepsilon\sqrt{\frac{X}{|Y|}}\cos k_c x \qquad (4.13)$$

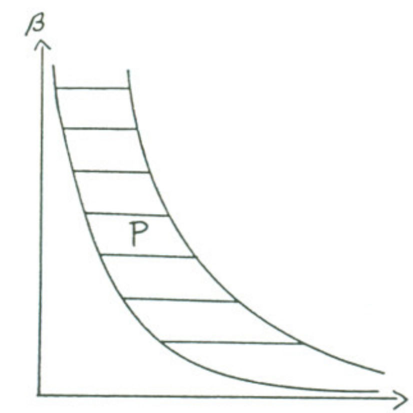


**Figure 2.** Parameter space P, (shaded), where $Y > 0$ ((4.12)) and the homogeneous steady state $n(x,t) = 1$ evolves to the heterogeneous solution (4.13).

If we include all of the initial constants, we would have finished up with the perturbed version of the above Landau equation, namely

$$\frac{dA_1^0(T)}{dT} = C_0 + \delta(X+X_0)A_1^0(T) + Z_0\{A_1^0(T)\}^2 + Y\{A_1^0(T)\}^3 \qquad (4.14)$$

where $C_0$, $X_0$ and $Z_0$ are functions of $\gamma_1^i$ and $\gamma_3^i$, $i = 0,1$.

In this case the homogeneous steady state would evolve to a heterogeneous steady state dependent on initial perturbations. As we are dealing with small perturbations, these variations are small.

## 5. Two-Dimensional Nonlinear Analysis.

In this section we analyze a caricature of the above model (3.1) in which (3.1a) involves only convection and consider it in two dimensions to investigate the possibility of a regular tesselation pattern. We linearise the conservation equations $\frac{\partial n}{\partial t} + \nabla\cdot(n\frac{\partial \underline{u}}{\partial t}) = 0 = \frac{\partial \rho}{\partial t} + \nabla\cdot(\rho\frac{\partial \underline{u}}{\partial t})$ about the steady state $n = \rho = 1$, $\underline{u} = \underline{0}$ which on integration give

$$n = 1 - \theta, \ \rho = 1 - \theta \qquad (5.1)$$

where $\theta = \operatorname{div} \underline{u}$, and in which we assume $\theta < 1$ as n and $\rho$ are necessarily non-negative.

We replace the $su\rho$ term in the mechanical balance equation by the linearised term $s\underline{u}$ and take the divergence of the resulting equation. Using the identity $\nabla\cdot\varepsilon = \text{grad div } \underline{u} - \frac{1}{2} \text{curl curl } \underline{u}$ for the divergence of the linear strain tensor, the equation becomes

$$\nabla^2 \frac{\partial\theta}{\partial t} + \nabla^2\theta + \tau\nabla^2\{[1-\theta]^2 - \beta[1-\theta]\nabla^2\theta\} - s\theta = 0 \qquad (5.2)$$

Clearly the dispersion relation for this equation is (4.2) and for $\tau > \tau_c$, where $\tau_c$ is given by (4.3), the uniform steady state is linearly unstable. To study the full nonlinear system, we substitute

$$\tau = \tau_c + \sum_{i=1} \varepsilon^i \tau_i, \ \theta(\underline{x},t) = \sum_{i=1} \varepsilon^i \theta_{i-1}(\underline{x},t) \ \text{ where } 0 < \varepsilon < 1 \qquad (5.3)$$

into equation (5.2). As in section 4, this gives rise to a hierachy of linear



equations which we can solve. We follow in part the process used by Busse (1983).

The only regular patterns in the plane are rolls, triangles (hexagons), squares, and tesselations of these. Therefore we look for $\theta_0(\underline{x},t)$ of the form

$$\theta_0 = \frac{1}{2} a_1(t)\{\cos(kx + ly) + \cos(ly - kx)\} + a_2(t)\cos 2ly \qquad (5.4)$$

where the fastest growing unstable mode has wave number $\kappa$ (= $(s/\beta\tau_c)^{1/4}$) and $k^2 + \ell^2 = \kappa^2$, $4\ell^2 = \kappa^2$. Putting $a_1(t) = 0$, $a_2(t) = 0$, $a_1(t) = 2a_2(t)$ into (5.4) gives roll, rhombic and hexagonal structures respectively (Christopherson (1940)).

With $\theta_0(\underline{x},t)$ as above, $\theta_1(\underline{x},t)$ must have the form

$$\theta_1 = b_1(t)\cos 4ly + b_2(t)\cos(3ly+kx) + b_3(t)\cos(3ly-kx)$$
$$+ b_4(t)\cos 2(ly+kx) + b_5(t)\cos 2(ly-kx) + b_6(t)\cos 2kx$$

where, on equating coefficients of $\varepsilon^2$, we can find $b_i(t)$, $i = 1, 2\ldots6$ in terms of $a_1(t)$ and $a_2(t)$: it is a simple but tedious calculation.

Taking powers of $\varepsilon$ up to $\varepsilon^3$ into account, to suppress secular terms $a_1(t)$ and $a_2(t)$ must satisfy the coupled system of ordinary differential equations

$$\kappa^2 \frac{da_1(t)}{dt} = Xa_1(t) - Ya_1(t)a_2(t) - 2Za_1(t)a_2{}^2(t) - \frac{1}{4}(2Z+R)a_1{}^3(t)$$
$$\kappa^2 \frac{da_2(t)}{dt} = Xa_2(t) - \frac{Y}{4}a_1{}^2(t) - Za_1{}^2(t)a_2(t) - Ra_2{}^3(t) \qquad (5.5)$$

where $X = \frac{(2\tau_c+1)}{2\tau_c}\{\varepsilon\tau_1+\varepsilon^2\tau_2\}\kappa^2$, $Y = \frac{1}{2\tau_c}\{\varepsilon\tau_c+\varepsilon^2\tau_1\}\kappa^2$,

$$Z = \frac{3\varepsilon^2}{16\beta\tau_c}\{\tau_c-1\} \text{ and } R = \frac{\varepsilon^2}{36\beta\tau_c}\{6\tau_c-5\}.$$

We can take $\tau_1 > 0$, thus X and Y are positive and the sign of R and Z depend on the value of $\tau_c$.

The system (5.5) has the following steady states

$$\text{I. } a_1 = a_2 = 0;$$

$$\text{II. a,b } \; a_1 = 0,\; a_2 = \pm\sqrt{X/R}$$

$$\text{III. a,b } \; a_1 = 2a_2,\; a_2 = \frac{-Y\pm\sqrt{Y^2+4X(4Z+R)}}{2(4Z+R)}; \qquad (5.6)$$

$$\text{IV. a,b } \; a_1 = -2a_2,\; a_2 = \frac{-Y\pm\sqrt{Y^2+4X(4Z+R)}}{2(4Z+R)};$$

$$\text{V. a,b } \; a_1 = \frac{\pm 2\sqrt{X-\frac{RY}{R-2Z}}}{\sqrt{R+2Z}},\; a_2 = \frac{Y}{R-2Z}$$

where, for example, IIa,b exists if and only if $\tau_c > \frac{5}{6}$. Note that to lowest order in $\varepsilon$, IIIa is $a_1 = 2a_2$, $a_2 = \frac{-Y_0+\sqrt{Y_0^2}}{2(4Z+R)} = 0$, where $Y_0 = \frac{\varepsilon}{2}\kappa^2$, and this is the same as I. A similar argument can be applied to IVa and, in the following analysis, we will not distinguish between states I, IIIa and IVa.

We can analyze the stability of states I-IV in (5.6) by calculating the eigenvalues ($\lambda_s$) of the appropriate matrix. This gives a quadratic for $\lambda_s$, with coefficients dependent on $\varepsilon$. To simplify the solution of the quadratic we approximate the coefficients to lowest order in $\varepsilon$. Table 3 summarises the results of the stability analysis.

Table 3. Summary of stability analysis of the steady states I-IV (5.6) of the coupled system of ordinary differential equations (5.5).

| $\tau_c < 5/6$ | $5/6 < \tau_c < 47/51$ | $47/51 < \tau_c < 32/33$ | $\tau_c > 32/33$ |
|---|---|---|---|
| I unstable star | | | |
| IIa,b do not exist | IIa stable node<br>IIb saddle point | | |
| IIIb and IVb unstable node | | IIIb and IVb saddle point | IIIb and IVb stable node |

Note that for $\frac{5}{6} < \tau_c < \frac{32}{33}$ the only stable regular pattern is a roll, while for $\tau_c > \frac{32}{33}$ rolls and hexagons are stable. In the latter case, the evolved pattern depends on initial conditions.



## 6. Biological Application to the Formation of Skin Organ Primordia.

In the early stages of skin organ development (hair, teeth, feathers, scales) dermal cells aggregate to form a regular spatial pattern. These aggregations (papillae), in association with overlapping arrays of columnar epidermal cells (placodes), lead to the formation of skin organ primordia (e.g. Rawles (1963), Wessels (1965)).

Rows of feather primordia develop sequentially to form a hexagonal pattern within well-defined regions of chicken skin (pterylae). The pattern is initiated by a single row of feather primordia forming along the dorsal midline in the posterior part of the spinal pteryla (Stuart and Moscona (1967), Davidson (1983)) and successive rows form on either side of this initial row.

We apply our model to this with the following scenario: initially there is a uniform density of dermal cells along the dorsal midline. As the cell traction increases (or other parameters involved in the dimensionless traction parameter change appropriately) this homogeneous steady state bifurcates into a heterogeneous pattern of isolated clumps (cf. section 4). This parameter evolution may be due, for example, to cell maturity: cells "age" into the unstable regime in parameter space. The tractions produced by these aggregates strain the matrix and a secondary row of papillae are encouraged to form at loci midway between the primary papillae, where the strain is a local minimum. This recruits other cells and thereby forms a hexagonal pattern. The scenario is illustrated in Figure 3.

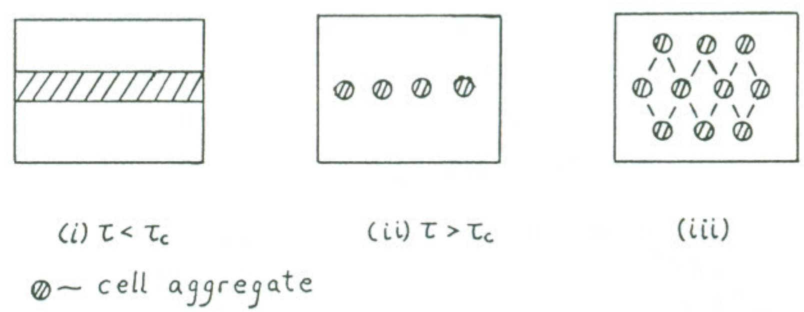


**Figure 3.** Scenario for hexagonal pattern formation in an idealized section of chick pteryla. As traction increases, the uniform cell density (i) becomes unstable and evolves into a row of isolated aggregations (ii); this sets up a strain field causing condensations along a neighbouring row at intermediate points; (iii) illustrates how hexagonal patterns can arise.

## 7. Conclusions.

We have presented a model for cell aggregation based on well documented mechanical properties of cells and extracellular matrix. We have illustrated how cell traction on a viscoelastic substratum can produce aggregations in one- and two-dimensions. Two dimensional patterns may be produced synchronously (section 5) or asynchronously (section 6). No directed cell migration is necessary. Numerical simulations (in one dimension) of the full equations (to be presented elsewhere) show the aggregation patterns. Numerical studies are underway to verify the two-dimensional patterns.

In this model, the extracellular matrix behaves as a passive viscoelastic material. However, in cartilage formation in chick limbs, the osmotic component of the extracellular matrix plays an active role in aggregation formation (Oster, et al (1985)). Some of the predictions made by these mechanical models can be (and are being) investigated experimentally.

**Acknowledgements:** P. K. Maini and J. D. Murray would like to thank the Mathematics Department, University of Utah for supporting a visit during which some of this research was carried out. P. K. Maini wishes to thank the Department of Education of N. Ireland for a postgraduate studentship. G. F. Oster was supported by NSF grant #MCS-8110557. G. F. Oster would also like to acknowledge support from the Science and Engineering Research Council of Great Britain (grant GR/c/63595) for a visit to the Centre for Mathematical Biology in Oxford.



## APPENDIX

(A.1) To non-dimensionalise the model (2.1a)-(2.1c), let $L$ and $T_0$ by typical length and time scales respectively and let $\rho_0$ be a typical matrix density. The dimensionless quantities are

$$\tilde{\underline{x}} = \frac{\underline{x}}{L}, \quad \tilde{t} = \frac{t}{T_0}, \quad \tilde{n}(\tilde{\underline{x}},\tilde{t}) = \frac{n(\underline{x},t)}{N}, \quad \tilde{\rho}(\tilde{\underline{x}},\tilde{t}) = \frac{\rho(\underline{x},t)}{\rho_0}, \quad \tilde{\underline{u}}(\tilde{\underline{x}},\tilde{t}) = \frac{\underline{u}(\underline{x},t)}{L},$$

$$\tilde{D}_1 = \frac{D_1T_0}{L^2}, \quad \tilde{D}_2 = \frac{D_2T_0}{L^4}, \quad \tilde{\lambda} = \lambda N^2, \quad \tilde{\beta} = \frac{\beta}{L^2}, \quad \tilde{s} = \frac{s\rho_0L^2(1+\nu)}{E}, \quad \tilde{\alpha} = \frac{\alpha\rho_0T_0}{L^2},$$

$$\tilde{r} = rNT_0, \quad \tilde{\mu}_1 = \frac{\mu_1(1+\nu)}{T_0E}, \quad \tilde{\mu}_2 = \frac{\mu_2(1+\nu)}{T_0E}, \quad \tilde{\tau} = \frac{\tau N\rho_0(1+\nu)}{E}$$

Dropping the tildes, the model system reduces to (3.1a)-(3.1c).

(A.2) The dispersion relation satisfied by the linear growth rate $\sigma(k^2)$ is

$$\sigma(k^2) = 0; \quad \text{or} \quad \sigma(k^2) = \frac{-b(k^2) \pm \sqrt{b^2(k^2) - 4\mu k^2c(k^2)}}{2\mu k^2}$$

where $b(k^2) = \mu D_2k^6 + \{\frac{\tau\beta}{(1+\lambda)} + \mu D_1\}k^4 + \{1 + \mu r - \frac{2\tau}{(1+\lambda)^2}\}k^2 + s$ and

$$c(k^2) = \frac{\tau\beta}{(1+\lambda)} D_2k^8 + \{(\frac{\tau}{1+\lambda})[\beta D_1 - D_2] + D_2\}k^6$$

$$+ \{(\frac{\tau}{1+\lambda})[r\beta - D_1 - \alpha(1-\frac{2\lambda}{1-\lambda})] + sD_2 + D_1\}k^4$$

$$+ \{sD_1 + r - \frac{r\tau}{(1+\lambda)}\}k^2 + rs$$

where $\mu = \mu_1 + \mu_2$ and we have divided $\mu$, $\tau$ and $s$ by $(1+\hat{\nu})$.

## REFERENCES


[1] Busse, F. H. (1983). Patterns of bifurcations in plane layers and spherical shells, in Modelling of Patterns in Space and Time (ed. W. Jager & J. D. Murray, (1984)) Proceedings, Springer-Verlag, Heidelberg. pp 51-60.

[2] Christopherson, D. G. (1940). Note on the vibration of membranes. Quart. J. of Math., 11, 63-65.

[3] Davidson, D. (1983). The mechanism of feather pattern development in the chick. 1. The time determination of feather position. J. Embryol. Exp. Morph., 74, 245-259.

[4] Harris, A. K. (1973). Behaviour of cultured cells on substrata of variable adhesiveness. Exp. Cell Res., 77, 285-297.

[5] Harris, A. K., Stopak, D. & Wild, P. (1981). Fibroblast traction as a mechanism for collagen morphogenesis. Nature, 290, 249-251.

[6] Lara Ochoa, F. & Murray, J. D. (1983). A non-linear analysis for spatial structure in a reaction diffusion model. Bull. Math. Biol. 45, 917-930.

[7] Maini, P. K., Murray, J. D. & Oster, G. F. (1985). A mechanical model for biological pattern formation: A nonlinear bifurcation analysis. Dundee Conference (1984) on "Partial and Ordinary Differential Equations." (to appear in the proceedings.) Springer-Verlag, Heidelberg.

[8] Matkowsky, B. J. (1970). A simple non-linear dynamic stability problem. Bull. Amer. Math. Soc., 620-625.

[9] Meinhardt, H. (1982). Models of biological pattern formation. Academic Press, London.

[10] Murray, J. D. (1977). Lectures on non-linear differential equation models in biology. Oxford University Press: Oxford.

[11] Murray, J. D. (1981 a). On pattern formation mechanisms for Lepidopteran wing patterns and mammalian coat markings. Phil. Trans. Roy. Soc. Lond. B295, 473-496.

[12] Murray, J. D. (1981 b). A pre-pattern formation mechanism for animal coat markings. J. Theor. Biol., 88, 161-199.

[13] Murray, J. D. & Oster, G. F. (1984 a). Generation of biological pattern and form. I. M. A. J. Maths. Appl. to Biol. & Med., 1, 51-75.

[14] Murray, J. D. & Oster, G. F. (1984 b). Cell traction models for generating pattern and form in morphogenesis. J. Math. Biol., 19, 265-279.

[15] Odell, G., Oster G. F., Burnside, B. & Alberch, P. (1981). The mechanical basis of morphogenesis I: Epithelial folding and invagination. Devl. Biol., 85, 446-462.





[16] Oster, G. F., Murray J. D. & Harris, A. K. (1983). Mechanical aspects of mesenchymal morphogenesis. J. Embryol. Exp. Morph. 78, 83-125.

[17] Oster, G. F., Murray, J. D. & Maini, P. K. (1985). A model for chondrogenic condensations in the developing limb: The role of extracellular matrix and cell tractions. J. Embryol. Exp. Morph. (to appear).

[18] Purcell, E. M. (1977). Life at low Reynolds number. Amer. J. of Phys., 45, 3-11.

[19] Rawles, M. (1963). Tissue interactions in scale and feather development as studied in dermal-epidermal recombinations. J. Embryol. Exp. Morph., 11, 765-789.

[10] Stuart, E. S. & Moscona, A. A. (1967). Embryonic morphogenesis: Role of fibrous lattice in the development of feathers and feather patterns. Science, 157, 947-948.

[21] Tickel, C., Summerbell, D. & Wolpert, L. (1975). Positional signalling and specification of digits in chick limb morphogenesis. Nature Lond., 254, 199-202.

[22] Trinkaus, J. P. (1984). Cells into organs: The forces that shape the embryo. (Prentice-Hall).

[23] Turing, A. M. (1952). The chemical basis of morphogenesis. Phil. Trans. Roy. Soc. Lond., B237, 37-73.

[24] Wessels, N. K. (1965). Morphology and proliferation during early feather development. Dev. Biol., 12, 131-153.

[25] Wolpert, L. (1969). Positional information and the spatial pattern of cellular differentiation. J. Theor. Biol., 25, 1-47.

[26] Wolpert, L. (1981). Positional information and pattern formation. Phil. Trans. Roy. Soc. Lond. B295. 441-450.

[27] Wolpert, L., Hicklin, J. S. Hornbruch, A. (1971). Positional information and pattern regulation in regeneration of hydra. Symp. Soc. exp. Biol., 25, 391-415.